

Low Intensity Gamma-Ray Spectroscopy of the Lake Labyrinth Meteorite

A Senior Project

By

Tristan C. Paul

Advisors: Dr. Grismore, Dr. Klay

Department of Physics, California Polytechnic University San Luis Obispo

September 3, 2015

Approval Page

Title: Low Intensity Gamma-Ray Spectroscopy of the Lake Labyrinth Meteorite

Author: Tristan C. Paul

Date Submitted: September, 2015

Senior Project Advisors: Dr. Grismore, Dr. Klay

Signature

Date

Abstract

A 23.7g fragment of the Lake Labyrinth Meteorite (fell in 1924, collected in 1934 at Lake Labyrinth in South Australia, Australia) was re-investigated for evidence of the presence of ^{98}Tc using a two dimensional low-intensity gamma-ray spectrometer. A new calibration technique using ^{26}Al sources found the gamma-rays previously thought to be due to ^{98}Tc are more likely from ^{166}Ho . The presence of ^{166}Ho is most likely due to activation of the stable ^{165}Ho in the meteorite from terrestrial background sources where it was stored.

Acknowledgements

I would first like to give my unending thanks to the late Roger Grismore. His love of working with students and his pride in working with them was readily apparent the first day I met him. One of his favorite stories was how a student convinced him to switch from using the gamma-ray spectrometer for measuring radiation in fish to partnering with NASA to study meteorites. His patience and flexibility as I second guessed all my analysis and broke my arm was amazing. I do not think there is a greater compliment than saying that when I am in my nineties, I hope to have half the energy he did and to still be involved with physics as he was.

Second, I would like to thank Jennifer Klay. She has been the perfect guide and mentor for me; always giving me a gentle but firm push to take an extra step so that my best can become even better. This paper has immensely benefited from her ability to take the words I wrote and coax them into the phrases that I was trying to write. I cannot thank her enough for becoming my senior project advisor without any hesitation despite being incredibly busy after Dr. Grismore passed away. The fact that she still remembers meeting me as a wide-eyed college applicant with so many questions that I couldn't voice any of them speaks volumes about her care for her students. She too is the sort of physicist and person that I hope I can be.

I'd also like to thank my parents, Mom, Hugh, Dad, and Jill. I would not be where I am today without their unconditional love and support. They always believed in me and made sure I was safe and well. They made sure I got the very best education I possibly could and always helped me when I struggled. Their impact on my life is immeasurable in its goodness and size.

Finally I'd like to thank my girlfriend Esther. She has cared for me and dealt with my insanities for almost eight years and I love her for it. She has kept my ADHD-fueled mind organized and grounded so I have been able to do my very best in everything.

Contents

1	Introduction	7
2	Theory	8
3	Detector and Experimental Set-up	9
3.1	The Spectrometer	9
3.1.1	Scintillation Crystal	9
3.1.2	Detectors	9
3.1.3	Signal Path	10
3.1.4	Data Storage	11
3.2	Consequences of Configuration	12
3.2.1	Coincidences	12
3.2.2	Compton Smearing	12
4	Procedure	13
4.1	Proper Usage and Contamination Avoidance	13
4.2	Calibration of Baseline and Gain	14
4.3	Data Runs	15
5	Analysis	16
6	Conclusion	21
7	Additional Figures	22

List of Tables

1	Possible combinations of photon arrivals into the detectors and how the spectrometer stores the event. An X indicates a photon trigger of a detector.	13
2	Baseline and gain calibration gamma-rays.	14
3	Settings for calibration runs.	15

4	Average gain and baseline adjustment guidelines for each detector. These numbers represent the average amount a scale dial must be rotated to achieve a change of one channel on the ADC. The amount of rotation is measured by the smallest division markings on the scale dials.	15
5	Measured energies for each valid peak and the possible sources. Easily eliminated possible sources are excluded to save space. Reflected peaks are listed with the same number and differentiated by an a or b.	20

List of Figures

1	A simplified representation of the gamma-ray spectrometer.	10
2	A box diagram of signal paths of the spectrometer.	11
3	An example of a fitted peak from the MatLab code. The peak shown is the annihilation peak from ^{26}Al with a coincidence between two 511 keV gamma-rays. The data is represented by the dots while the fit is shown with the contour.	17
4	Background subtracted Data. Blue corresponds to few to no counts and red to most counts. Note that channels 0 through 10 from each detector were removed from this plot. These lower channels represent backgrounds that were not analyzed in this project. . . .	18
5	Fitted channel-to-energy curves for the upper and lower detectors.	19
6	The peaks suspected to be caused by ^{98}Tc decay.	21
7	^{26}Al Peaks used for calibration from the non-background subtracted sample run	22
8	^{26}Al Peaks used for calibration from the background run	23
9	Analyzed peaks from Table 5.	24

1 Introduction

The Lake Labyrinth meteorite was discovered by Billy Austin shortly after it fell, likely on February 5, 1924. Two fragments were removed at that time. Austin then guided R. Bedford back to the landing site in 1934 at which time a majority of the remaining meteorite was collected. The meteorite was estimated to weigh 75 lbs, 57 lbs of which were collected. At the time of collection in 1934, the meteorite was heavily fragmented. Bedford estimated the location of the impact to be $30^{\circ} 20' S$, $134^{\circ} 45' E$. Bedford gave some of the fragments to the British Museum with the request that it be named the Lake Labyrinth Meteorite [1]. Dr. Roger Grismore obtained a 23.7g fragment of the Lake Labyrinth meteorite which has the designation M79.3 to investigate for any unusual radioactivities [2].

The goal of this project was to identify whether or not the Lake Labyrinth meteorite contained the extinct radionuclide ^{98}Tc . An extinct radionuclide is a radionuclide that is believed to have been created during stellar nucleosynthesis prior to the formation of the solar system, but is no longer present. These radionuclides have half-lives that can reach hundreds of millions of years. Such a time frame is short in comparison to the 4.6 billion years since the creation of the solar system, thus the extinct radionuclides should have all decayed away leaving only their daughter nuclides [3].

The presence of an extinct radionuclide, ^{26}Al , was found using a two-dimensional anti-coincidence shielded low intensity gamma-ray spectrometer by Grismore and student Aaron Ginn in a previous senior project [4]. Since the half-life of ^{26}Al is 7.15×10^5 years, it could not have been made by local stellar nucleosynthesis. The ^{26}Al may have been synthesized by a nearby red giant star and blown into the solar system [5]. ^{99}Tc can also be produced via gamma-ray induced fission in red giants and then undergo (d,p) or (n,t) reactions to produce ^{98}Tc [6]. Thus if the ^{26}Al was produced this way, ^{98}Tc should also be present.

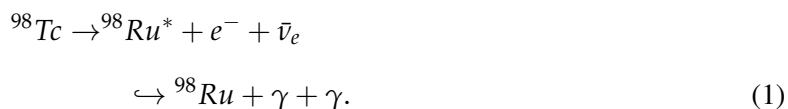
The radioactive contents of the Lake Labyrinth meteorite were previously investigated in a senior project by Kristopher Merolla and a peak that could indicate the presence of ^{98}Tc was found [7]. However, the energy of the peak could not be sufficiently resolved with the calibration used at the time. This paper presents a re-examination of the Lake Labyrinth meteorite using a new calibration technique utilizing the ^{26}Al peaks that were found previously in meteorites by Grismore and Ginn [4]. This paper also presents the methods and procedures of low intensity gamma-ray spectrometry using a coincidence

shielded, two-dimensional spectrometer.

2 Theory

Radionuclides are unstable due to excess energy in the nucleus. Eventually the unstable nucleus undergoes radioactive decay to reach a lower and more stable energy state. The energy from the de-excitation of the nucleus can be emitted through high energy photons called gamma-rays, α -particle, β -particles, and other subatomic particles. This experiment takes advantage of decays that produce gamma-rays.

The decay route for ^{98}Tc that may be the source of the coincidence gamma-rays that are the subject of this project is



Here, ^{98}Tc undergoes β^- decay into an excited ^{98}Ru state. β^- decay is where a neutron decays into a proton, electron, and anti-electron neutrino. The excited ^{98}Ru nucleus then de-excites releasing two gamma-rays with energy 745.5 keV and 652.4 keV, respectively.

The main decay route of ^{26}Al is β^+ decay, described by



This process is the opposite of β^- decay. A proton in the nucleus of ^{26}Al becomes a neutron by releasing a positron and an electron neutrino. The nucleus, now an excited ^{26}Mg nucleus, de-excites by releasing an 1809 keV gamma-ray. The positron will quickly annihilate with an electron after it is emitted. Annihilation,



produces two gamma-rays, both with 511 keV of energy. The spectrometer can detect five different coincidences from ^{26}Al decay which will be described in section 5.

3 Detector and Experimental Set-up

3.1 The Spectrometer

The detector used for this project was a two-dimensional anti-coincidence shielded low intensity gamma-ray spectrometer built by Roger Grismore at Cal Poly San Luis Obispo in the early 90's. This spectrometer consists of two primary NaI(Tl) scintillation crystals each with a single photomultiplier tube (PMT) attached and an outer NaI(Tl) ring with eight evenly spaced PMTs attached. The spectrometer is run through the command prompt of a computer running Windows 98 and controlled by settings on modules along the signal path. Data is stored onto the computer's hard drive then backed up onto floppy drives at a later time.

3.1.1 Scintillation Crystal

The scintillation crystals are solid uncracked sodium iodide crystals doped with thallium. Gamma-rays that interact with the NaI(Tl) crystal are absorbed and excite electrons in the crystal to higher orbitals. The electrons de-excite and release an amount of light that is proportional to the amount of energy absorbed. It is important that the crystal is uncracked since cracks in the crystals cause reflections of the light. This would reduce the detector's efficiency, rendering it incapable of detecting the picocurie level radiation emitted by the samples in this experiment.

The thallium in the crystal allows it to act like a doped semiconductor. The thallium reduces the band gap energy of the pure sodium iodide crystal which increases the chances of electron stimulation in the crystal by a photon. Additionally, the altered band gap changes the wavelength of the photons emitted by the crystal. The NaI(Tl) crystal's emission wavelength is chosen to match the PMT's maximum sensitivity and to minimize the chance of reabsorption by the crystal.

3.1.2 Detectors

The light from the primary scintillation crystals are collected by single PMTs. The light from the ring is collected in eight PMTs equally spaced around it. The primary scintillators are oriented vertically and separated by one inch so as to form a cavity for the sample. The ring surrounds both the sample cavity and parts of the upper and lower detectors. A diagram of the spectrometer can be seen in Figure 1. The

entire spectrometer is surrounded by low radiation lead bricks to reduce background counts.

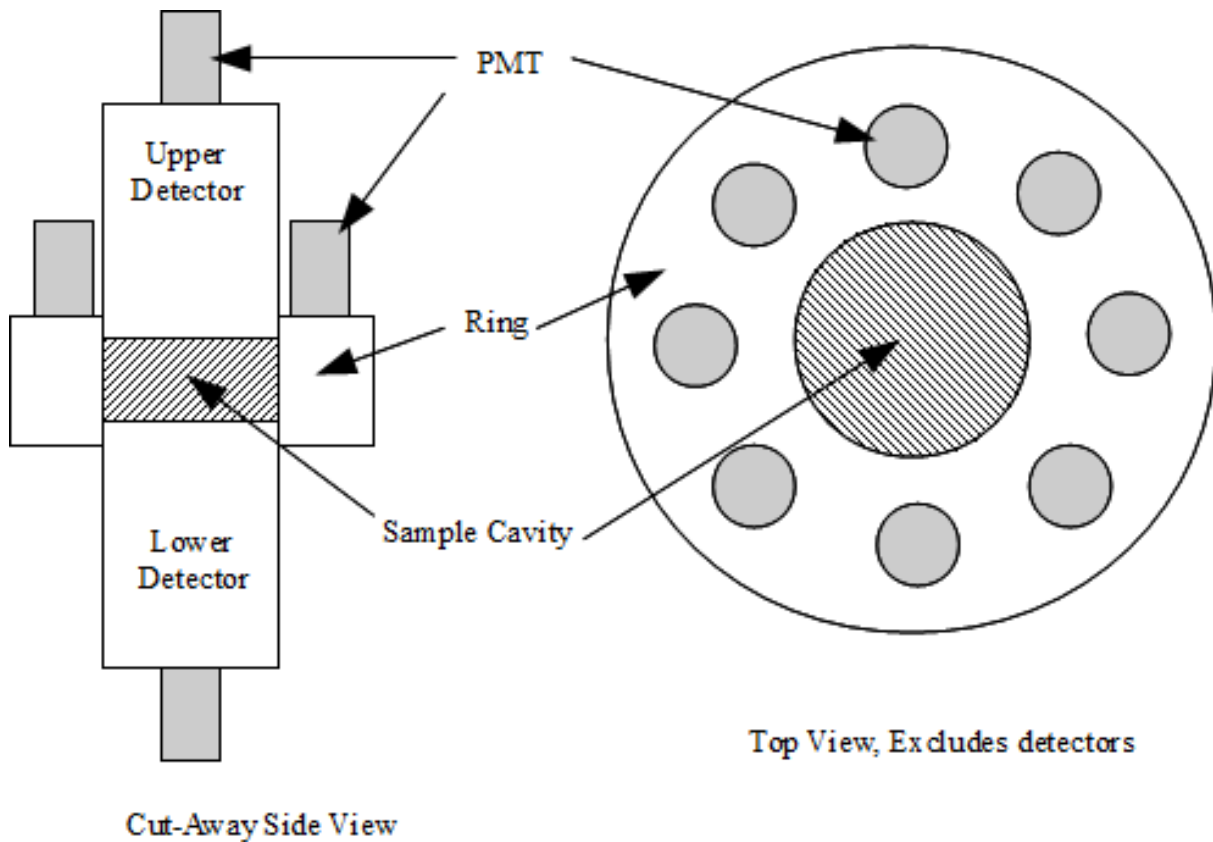


Figure 1: A simplified representation of the gamma-ray spectrometer.

3.1.3 Signal Path

The outputs from the PMTs are sent to pre-amplifiers (pre-amp). There is a single pre-amp for each PMT which is placed close to the PMT to minimize the signal's path length and thus reduce noise. Signals from the ring pass through dual sum and inverter amplifiers, and then an integrator unit which reduces noise. Finally the ring signals go to the coincidence checker which checks for coincidence between the ring and the main detectors. This is further described in section 3.2.2. The signals from the upper and lower detectors pass through separate amplification and discrimination units, pass through the coincidence checkers, go through Analog-to-Digital Converters (ADC), and then meet in a two parameter unit (TPU). The TPU determines how a count is stored in the computer that runs the spectrometer based

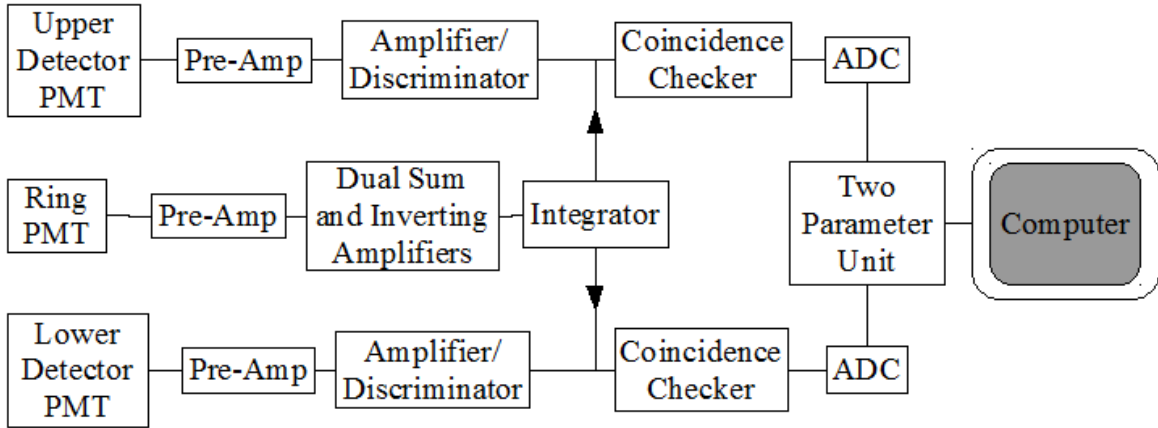


Figure 2: A box diagram of signal paths of the spectrometer.

on which mode the unit is operating in. These modes are described in section 3.2.1 and 4.2. Figure 2 depicts this setup [8].

3.1.4 Data Storage

The spectrometer primarily operates in the “XY + Singles” TPU mode. Operation in “XY + Singles” will be assumed unless stated otherwise for the rest of the paper. In this mode, the TPU discriminates between events detected by both main detectors within a set time limit (a coincidence event), and single detection events. For this experiment the coincidence limit was set to $2\mu\text{s}$.

Events are stored in a square table of ADC channels where each channel (Ch) correlates to photon energy deposited in a main detector (E) by the equation

$$Ch = G \times E + B. \quad (4)$$

G is the gain of the amplifier and B is the baseline of the ADC. Coincidence events are stored as a count at a position (x, y) where x is the upper detector channel and y is the lower detector channel. Single photon events are stored along the x -axis if the event is only in the upper detector and along the y -axis if it is only in the lower detector. Dead time corrected run time is stored at the origin. The table size is variable and chosen by the “Group Size” setting on the ADCs. Increasing the table size improves energy resolution, however it also decreases the number of counts at each position in the table. A decrease in

the number of counts in a position on the table leads to poor binning statistics and increased margins of error. The error for a counting experiment like photon detection goes as the square root of the number of counts, so more counts in a channel are desired. 126 x 126 (Group Size 128) was chosen to balance resolution and binning.

3.2 Consequences of Configuration

3.2.1 Coincidences

Coincidence events appear as a localized increase in counts, or peaks, in the table. Each coincidence peak, save those with equal energies deposited in both detectors, have a corresponding reflection peak about the $x = y$ line. This is the same peak, but the higher energy photon arrived in the opposite detector than did the lower energy photon. Corresponding peaks increase the distinction between random events and signal data.

Coincidence photons between the main detectors are used primarily because they are more likely to be emitted from the sample cavity rather than background sources. Background gamma-rays are unlikely to trigger both detectors within the set time frame.

The ring is set to anti-coincidence mode with the primary detectors to decrease effects of Compton Smearing (described in section 3.2.2) and decrease background counts as well. Anti-coincidence means that if the ring is triggered, any other event within the set coincidence time frame is removed from the data. Possible arrival combinations and how they are handled by the apparatus are shown in Table 1. Background gamma-rays are more likely to interact with the ring since the ring covers most of the sides of the primary detectors. These background reduction techniques, along with the lead brick casing, means the spectrometer has an average background count rate of only one count per channel per 24 hours.

3.2.2 Compton Smearing

When a gamma-ray from the sample is absorbed by one of the primary detectors, there is a chance that only some of the photon's energy is absorbed. The rest of the energy is re-emitted in a random direction as a second photon with less energy than the first. This effect is called Compton Scattering. Since only some of the energy is transferred to the NaI(Tl) crystal, the scintillators do not collect the full energy of

Upper	Lower	Ring	Response
X	X	X	Reject
X	X		Store
X			Store (x -axis)
X		X	Reject
	X		Store (y -axis)
	X	X	Reject
		X	Reject

Table 1: Possible combinations of photon arrivals into the detectors and how the spectrometer stores the event. An X indicates a photon trigger of a detector.

the original gamma-ray and the event is stored in a lower channel. This creates a smearing effect that trails behind a coincidence peak.

The ring is run in anti-coincidence mode to help reduce the Compton smearing. Anti-coincidence mode means that if the ring is triggered, any associated events are discounted. Photons that are Compton scattered out of a primary detector have a high likelihood of interacting with the ring due to the geometry of the ring and primary detectors. Therefore, using the ring to reject events reduces the number of photon events recorded and thus also minimizes the Compton smearing.

4 Procedure

4.1 Proper Usage and Contamination Avoidance

To prepare the detector for observations, proper care and consideration must be given to ensure the crystals remain uncracked, and the sample cavity is not contaminated by outside radioactive sources such as sweat¹. The upper detector must be lifted to insert the sample into the cavity. It is raised by a mechanical winch. The cable of the winch has a clear plastic square with two holes attached to it. The two holes go around two metal rods which act as guides to ensure that the upper detector is withdrawn vertically. The metal plate that has the metal rod inserts was accidentally turned when the detector was moved so the rod labeled left goes on the right and vice-versa. There are no negative effects on the spectrometer itself due to the rotation of the plate. When initially withdrawing the detector from the

¹Some nutrients our bodies need, such as potassium, are slightly radioactive. Potassium is very similar to sodium so some trace potassium leaves our body when we sweat, making our sweat slightly radioactive.

Source	Energy (keV)
^{60}Co	1325
^{60}Co	1173
^{137}Cs	661

Table 2: Baseline and gain calibration gamma-rays.

casing, the winch should be set to a low speed so that PMT wires do not get pulled out and the PMTs remain as undisturbed as possible. Once the detector has cleared the casing, the speed may be turned up slightly. The same is true for returning the detector back to its position.

Due to the high sensitivity of the detectors, even the small amount of radioactive potassium from sweat can contaminate the data. Therefore, gloves as well as long sleeves or a lab coat should be worn when inserting or removing samples. The detectors can be cleaned with rubbing alcohol in case of possible contamination.

4.2 Calibration of Baseline and Gain

Calibration of the upper and lower detectors must be done before each data run. The channel-to-energy correlation tends to drift slightly during long runs, so a common starting baseline and gain to every run is needed. Calibration is done using ^{60}Co and ^{137}Cs samples as gamma-ray sources. Table 2 shows the energies of the gamma-rays that are used for calibration. The calibration samples are stored in another room to ensure they do not contaminate a data run since they are relatively strong sources in comparison to the experimental samples. The calibration samples should not be left in the detector for the same reason. Extended exposure to the comparatively high intensity of radiation from the calibration sources may damage the detector.

The specific settings for the TPU, ADC, and coincidence checker that are used for calibration are shown in Table 3. The calibration runs are started by running MCAMPX.exe on the computer. The user is then prompted to input a file name for the spectrum and then a run time in minutes. Run times of 7 minutes are generally used.

Once a calibration run is complete, the gain and baseline for each primary detector must be calculated. This is done by running CALDSK.exe which prompts the user for a spectrum file name. Using the

Unit	Setting	Value
TPU	Mode	X + Y
ADC	Group Size	1024
	Conversion Gain	2048
Coincidence Checker	Coincidence	Anti-Coincidence
	Ring Input	Removed

Table 3: Settings for calibration runs.

given spectrum, the program displays the location of the three calibration peaks and the computed gain and baseline. The standard values for both detectors is 0.0 ± 0.1 for the baseline and 501.1 ± 1.0 for the gain. The gains and baselines are adjusted with scale dials. The scale dials for adjusting the baselines are labeled “Zero Level” on the ADCs and the scale dials for adjusting the gains are labeled “Fine Gain” on the amplifiers. Table 4 shows the average effect a change of a single scale dial division has on the gain or baseline of each detector. These values are used to quickly calculate how much a given scale dial needs to be rotated to achieve the standard starting values for the gain and baseline. After a second calibration run, more precise values of the effects of adjustment can be obtained by calculating the change in gain and baseline between the two calibration runs. Calibration runs continue following minor adjustments each time until the standard values are met. The ring does not require any calibration since it is only used to eliminate events.

Description	Small Divisions/Channel
Upper Gain	1.24
Lower Gain	1.78
Upper Baseline	3.14
Lower Baseline	3.43

Table 4: Average gain and baseline adjustment guidelines for each detector. These numbers represent the average amount a scale dial must be rotated to achieve a change of one channel on the ADC. The amount of rotation is measured by the smallest division markings on the scale dials.

4.3 Data Runs

After calibrating the baseline and gain, the TPU is returned to “XY + Singles.” The Group size is set to 128, conversion gain is set to 512, the ring inputs are plugged in, and the coincidence switch is returned

to “Coincidence.” The computer’s clock is then reset to verify its accuracy. While this set is not entirely necessary, it is done to double check the computer’s internal clock. The program that starts a data run is MCA126X126.exe. The program asks for run time and a file name for saving the data. Once every 24 hours the data is saved to the file in case of a power outage.

5 Analysis

Two 50,000 minute (approximately 35 days) runs were used in this experiment. Originally week-long runs were attempted, but the number of events was too low to properly analyze. The sample run was first. The sample run contained the Lake Labyrinth meteorite as well as six other meteorites that contain ^{26}Al . In the second run, the Lake Labyrinth meteorite was removed so a background spectrum could be obtained. Five coincidence peaks caused by pair annihilation and β^+ decay of ^{26}Al were used to calibrate the sample and background runs. One peak, 511 keV and 511 keV, is caused by the detection of both annihilation gamma-rays only. Two peaks, 511 keV and 1809 keV and its reflection, are caused by the detection of one annihilation gamma-ray and the β^+ decay gamma-ray. These two peaks are substantially smaller than the other three peaks since it is unlikely that only one annihilation gamma-ray is detected, given that they are emitted 180° apart due to conservation of momentum. The final two peaks, 2320 keV and 511 keV and its reflection, are caused by one detector absorbing a single annihilation gamma-ray and the other detector absorbing the β^+ gamma-ray and the other annihilation gamma-ray.

Peaks were fitted using a weighted fit in MatLab to a two dimensional Gaussian curve characterized by the equation

$$z(x, y) = a + be^{-c(x-x_0)^2}e^{-d(y-y_0)^2}, \quad (5)$$

where z is the number of counts, x is the upper detector channel, y is the lower detector channel, a is the vertical offset, b is the height of the curve centered at (x_0, y_0) , and c and d control the width of the peak in the x and y directions respectively. Figure 3 shows an example of a fitted peak.

Each of the five calibration peaks in the sample and background runs were fitted to Equation 5, and the fitted centers were used to adjust the background data run to match the sample data run. The adjustment was done using a quadratic transformation in MatLab. The adjusted background was then subtracted from the sample run leaving only the coincidence gamma-rays emitted by the Lake Labyrinth

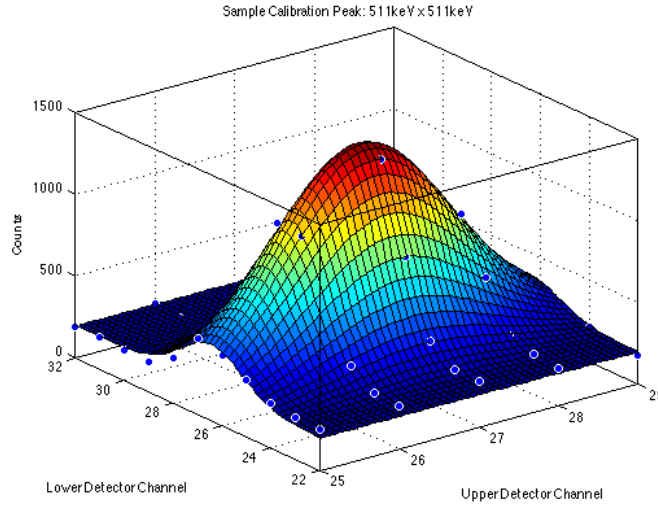


Figure 3: An example of a fitted peak from the MatLab code. The peak shown is the annihilation peak from ^{26}Al with a coincidence between two 511 keV gamma-rays. The data is represented by the dots while the fit is shown with the contour.

meteorite which is shown in Figure 4.

Two channel-to-energy conversions were required, one for the upper detector and one for the lower detector. Both were fitted to a quadratic equation using the detectors' respective calibration peaks (peaks with the 511 keV gamma-ray in the x -position for the upper detector and in the y -position for the lower detector). A quadratic calibration was chosen since NaI(Tl) crystal's output is almost linearly correlated to energy, but has a small quadratic effect. Figure 5 shows the calibration graphs. The energy of an upper detector event $E(x)$ in keV at a position x is given by

$$E(x) = -(0.0144 \pm 0.0003)x^2 + (21.49 \pm 0.05)x - (57 \pm 1.4), \quad (6)$$

and the energy of a lower detector event $E(y)$ in keV at a position y is given by

$$E(y) = -(0.0078 \pm 0.0004)x^2 + (20.52 \pm 0.05)x - (27 \pm 1.3). \quad (7)$$

Peaks were chosen by hand from the background subtracted sample data by looking for a localized increase in counts and a corresponding localized increase reflected about the $x = y$ line. The peaks were then fitted to Equation 5 and the energies of the coincidence gamma-rays were obtained by the calibration equations.

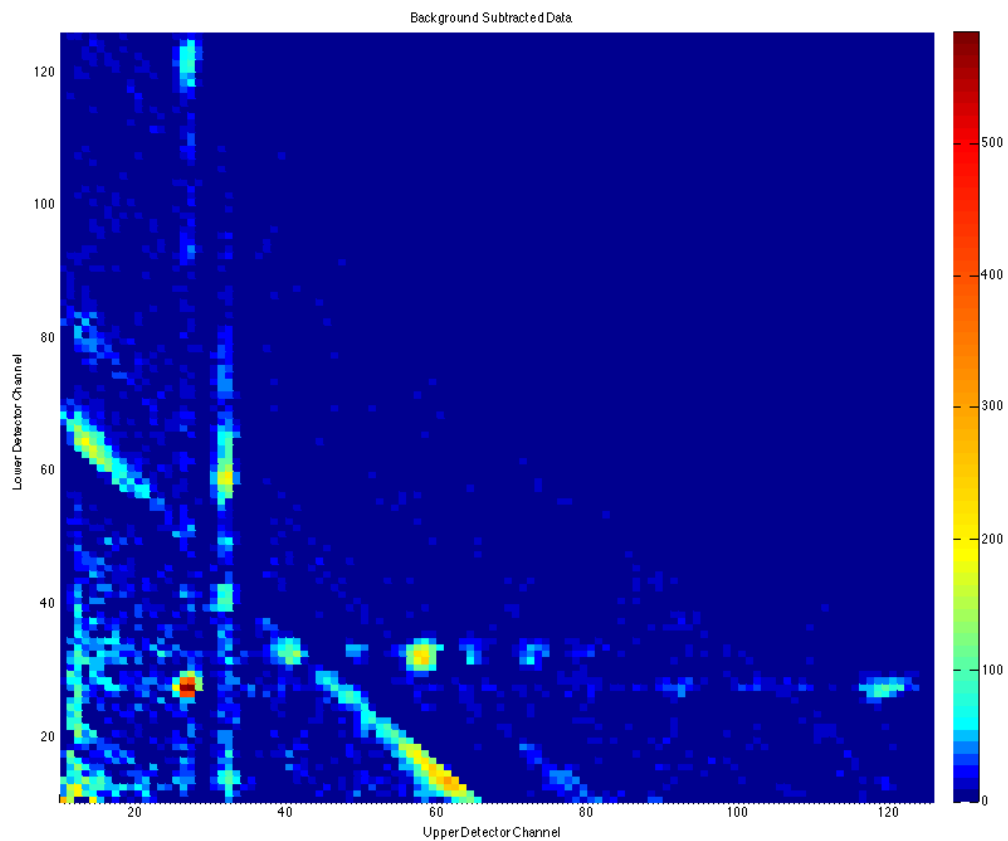
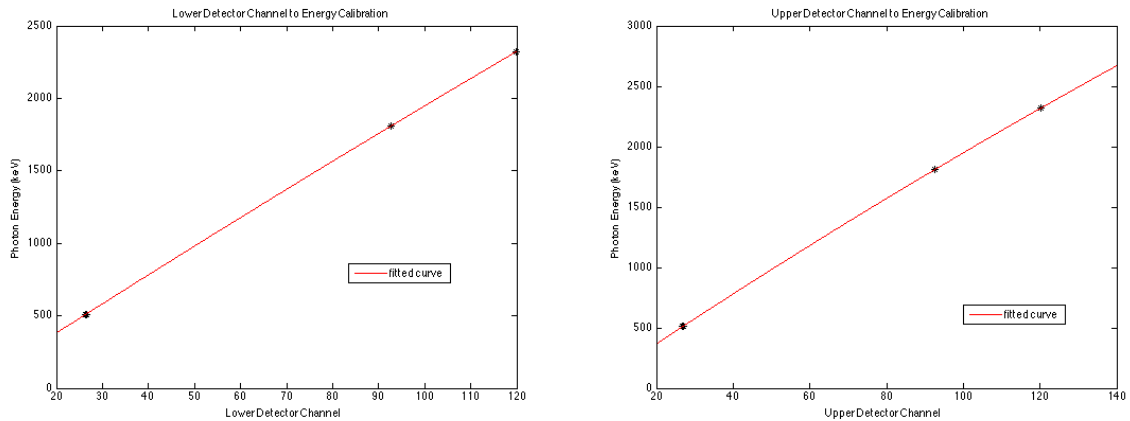


Figure 4: Background subtracted Data. Blue corresponds to few to no counts and red to most counts. Note that channels 0 through 10 from each detector were removed from this plot. These lower channels represent backgrounds that were not analyzed in this project.

The energies were put into NuDat, an online database of nuclear data [9]. NuDat’s Decay Radiation search was used to determine the nuclide that may have emitted them. The minimum and maximum energy of a gamma-ray to include in the NuDat search was determined by looking at the energies bounded by the value and error measured by each detector and setting the lower boundary to the smallest minimum and the upper boundary to the largest maximum. Only naturally occurring nuclides were included in the search and half-life was limited to at least 15 years. The restriction on half-life could be made since the Lake Labyrinth meteorite has been indoors for 90 years, reducing the exposure to solar and cosmic radiation. This means the contents of the meteorite have primarily been decaying and very few new radionuclides have been created. The remaining possibilities were then inspected based on intensity (what percentage of the total possible gamma-ray emission from the radionuclides are of the energy in question), and half-life. Low intensity coincidences were eliminated if the nuclide has a more probable decay that isn’t present in the data. The peaks, energies, and corresponding sources are shown in Table 5.



(a) Lower Detector Calibration

(b) Upper Detector Calibration

Figure 5: Fitted channel-to-energy curves for the upper and lower detectors.

The main peaks in question are 2a and 2b which were centered on points $(40.1 \pm 0.10, 32.2 \pm 0.10)$ and $(31.48 \pm 0.08, 40.4 \pm 0.15)$ in the table of channels. These peaks are shown in Figure 6. This run was carried out to verify if these peaks are due to ^{98}Tc undergoing β^- decay. The energies of the gamma-rays from ^{98}Tc are 745.5 keV and 652.4 keV which Equation 6 and Equation 7 predict to be centered near the points $(38, 38)$ and $(34, 33)$ on the table of channels. Former runs were not able to fully identify the

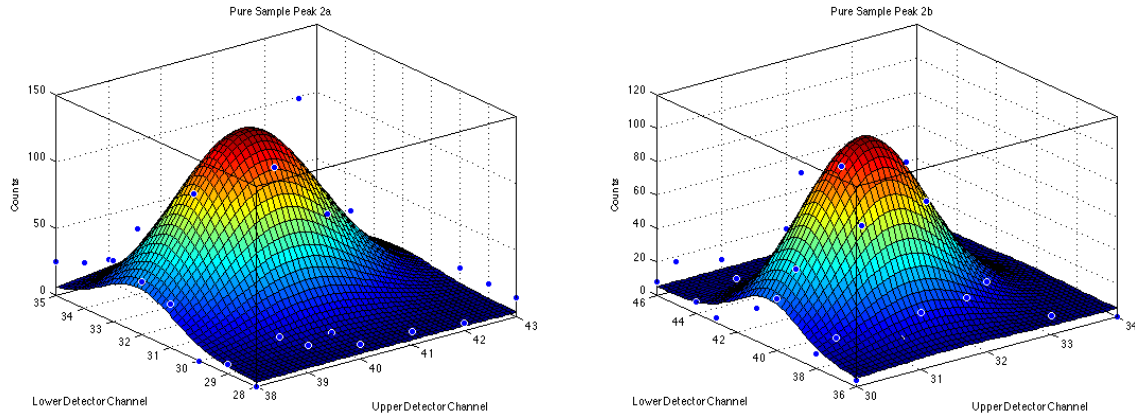
Peak	Upper Detector Energy (keV)	Lower Detector Energy (keV)	Possible Sources
1a	1131.7 ± 3.2	616.3 ± 2.3	^{158}Tb , ^{166}Ho
1b	607.1 ± 2.2	1151.6 ± 4.3	^{158}Tb , ^{166}Ho
2a	781.4 ± 3.2	625.2 ± 3.0	^{150}Eu , ^{166}Ho
2b	605.0 ± 2.6	790.4 ± 3.9	^{150}Eu , ^{166}Ho
3a	1189.8 ± 5.4	234.6 ± 3.9	^{166}Ho
3b	235.2 ± 4.2	1246.9 ± 5.8	^{166}Ho
4a	203.8 ± 4.4	610 ± 5.3	^{150}Eu , ^{166}Ho
4b	613.1 ± 2.6	253.0 ± 6.7	^{150}Eu , ^{166}Ho
5	502.3 ± 2.0	521.7 ± 2.0	Annihilation

Table 5: Measured energies for each valid peak and the possible sources. Easily eliminated possible sources are excluded to save space. Reflected peaks are listed with the same number and differentiated by an a or b.

sources which is why a new calibration technique using multiple ^{26}Al sources was implemented. This calibration technique successfully eliminated ^{98}Tc as a possible source.

The most probable source is ^{166}Ho . A previous Inductively Coupled Plasma Mass Spectrometry analysis carried out by Jon Friedrich at Purdue University indicated the presence of holmium in the meteorite [2]. The most abundant isotope of holmium is ^{165}Ho , which is stable. We speculate that the non-radioactive ^{165}Ho present in this sample was most likely activated through natural background neutron bombardment. The plastic scintillator used previously for the ring detector showed evidence of neutron capture. Since the detector and meteorite were stored together, the sample was probably activated by the same unknown neutron source. After the ring was replaced with the NaI(Tl) crystal, the neutron peak in the ring was no longer present.

It should be noted that after the data reduction processes were carried out to remove the background counts, the pure sample data had negative counts in some channels. The main cause of the negative peaks were imperfection in the quadratic transformation of the background run. Any negative counts in the data were forced to zero.



(a) Peak 2a, Higher energy gamma-ray detected by the upper detector

(b) Peak 2b, Higher energy gamma-ray detected by lower detector

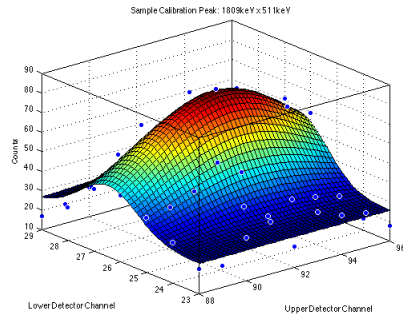
Figure 6: The peaks suspected to be caused by ^{98}Tc decay.

6 Conclusion

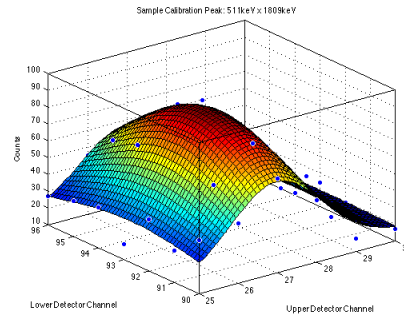
A 23.7g meteorite was investigated for the presence of ^{98}Tc using a two-dimensional coincidence shielded gamma-ray spectrometer. A previous analysis indicated the presence of ^{98}Tc , but better resolution of the photons' energies was required to properly identify the source of the radiation. This senior project utilized a new calibration technique to achieve the desired resolution.

^{26}Al decays in six previously measured meteorites created large peaks that were used to obtain a quadratic channel-to-energy calibration superior to the previous work. This calibration technique better resolved the gamma-ray peaks and ruled out ^{98}Tc as a source. Uncertainties could be further investigated by carrying out a χ^2 analysis of the fits, but such work was not conducted for this project. The source of the unknown gamma-ray peaks is most likely ^{166}Ho created by neutron activation of the naturally stable ^{165}Ho present in the Lake Labyrinth Meteorite.

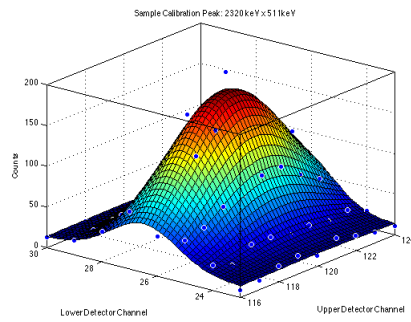
7 Additional Figures



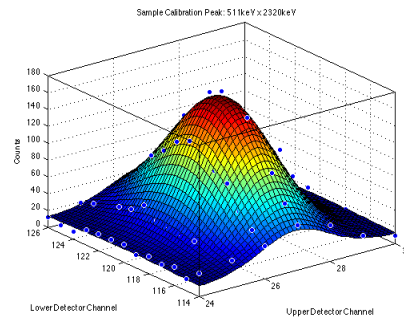
(a) 1809 keV Upper Detector, 511 keV Lower Detector



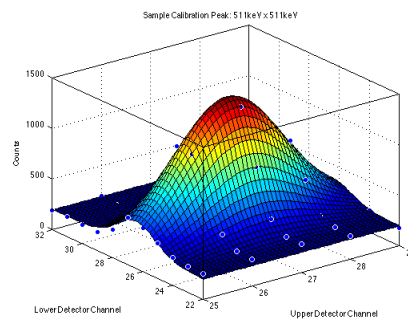
(b) 511 keV Upper Detector, 1809 keV Lower Detector



(c) 1809 keV and 511 keV Upper Detector, 511 keV Lower Detector

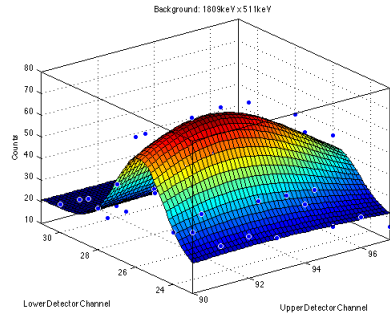


(d) 511 keV Upper Detector, 1809 keV and 511 keV Lower Detector

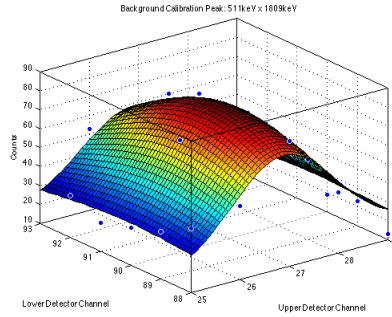


(e) 511 keV Upper Detector, 511 keV Lower Detector

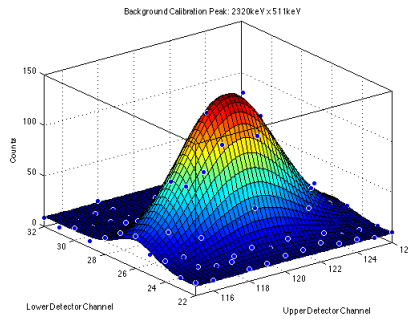
Figure 7: ^{26}Al Peaks used for calibration from the non-background subtracted sample run



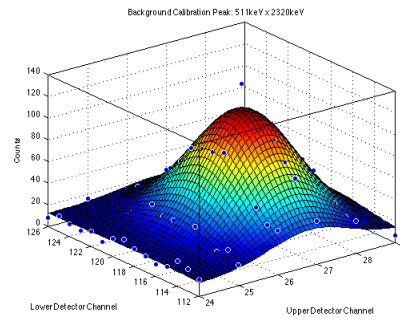
(a) 1809 keV Upper Detector, 511 keV Lower Detector



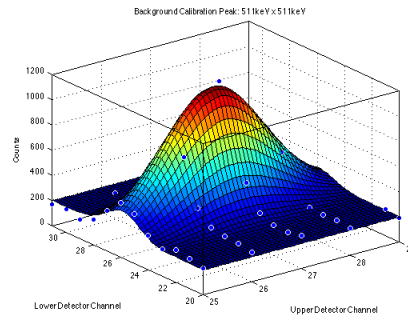
(b) 511 keV Upper Detector, 1809 keV Lower Detector



(c) 1809 keV and 511 keV Upper Detector, 511 keV Lower Detector

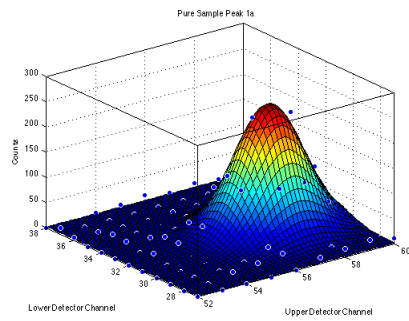


(d) 511 keV Upper Detector, 1809 keV and 511 keV Lower Detector

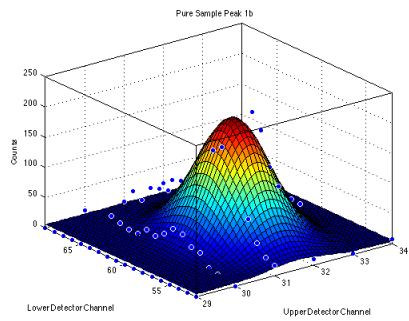


(e) 511 keV Upper Detector, 511 keV Lower Detector

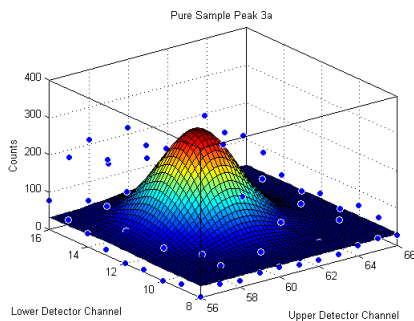
Figure 8: ^{26}Al Peaks used for calibration from the background run



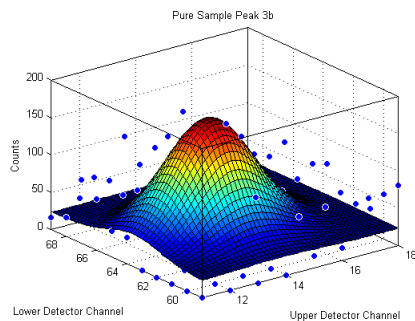
(a) Peak 1a



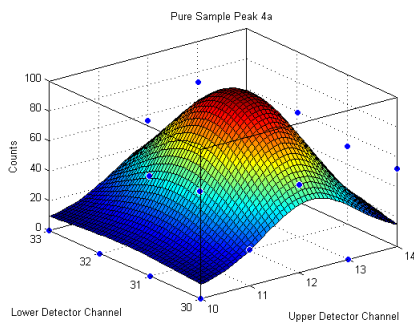
(b) Peak 1b



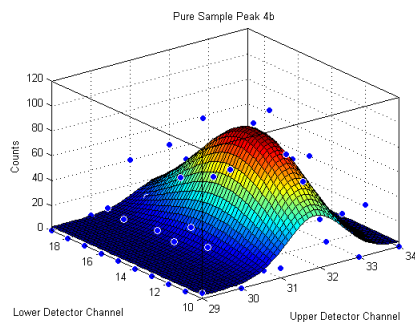
(c) Peak 3a



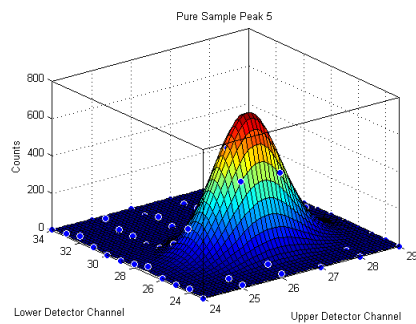
(d) Peak 3b



(e) Peak 4a



(f) Peak 4b



(g) Peak 5, annihilation peak

Figure 9: Analyzed peaks from Table 5.

References

- [1] L.J. Spencer, *Two New Meteoric Stones from South Australia - Lake Labyrinth and Kappakoola*,
- [2] J. M. Friedrich, Private correspondence between (1997).
- [3] *15 Extinct Radionuclides*. <http://www.onafarawayday.com/Radiogenic/Ch15/Ch15-1.htm>
- [4] A.S. Ginn, *gamma-ray Spectroscopy of Meteorite Samples with Attention to Assay of ^{26}Al* . California Polytechnic State University San Luis Obispo (1993).
- [5] N.Dauphas et al., *Short-lived p-nuclides in the early solar system and implications on the nucleosynthetic role of X-ray binaries*. Nucl.Phys. A719 (2003) 287-295
- [6] R. Malaney. *Production of technetium in red giants by gamma-ray-induced fission*. Nature (1998).
- [7] K.L. Merolla, *Gamma-Ray Spectroscopy: Meteorite Samples and the Search for ^{98}Tc* . California Polytechnic State University San Luis Obispo (2010).
- [8] G. Stratton, *Comparison of a High Purity Germanium gamma-ray Spectrometer and a Multidimensional NaI(Tl) Scintillation gamma-ray Spectrometer*. California Polytechnic State University San Luis Obispo (2011).
- [9] NuDat 2.6 <http://www.nndc.bnl.gov/nudat2/>